# Short-term earthquake probabilities during the L'Aquila earthquake sequence in central Italy, 2009

AGU FALL MEETING
San Francisco | 15–19 December 2014

S23A-4479

S23A: Aftershock Hazard: Forecasting Highly Time- and Space-Dependent Seismicity and Shaking after Large Mainshocks

G. Falcone[(1)], M. Murru[(1)], J. Zhuang[(2)], R. Console[(1,3)]

(1) Istituto Nazionale di Geofisica e Vulcanologia
(2) Istitute of Statistical Mathematics
(3) Centro di Geomorfologia Integrata per l'Area del Mediterraneo

e-mail:
giuseppe.falcone@ingv.it
maura.murru@ingv.it
zhuangjc@iism.ac.jp
rodolfo.console@ingv.it

Centro di Geomorfologia Integrata per l'Area del Mediterraneo
Research Organization of Information and Systems
The Institute of Statistical Mathematics
INGV terremoti vulcani ambiente
ISTITUTO NAZIONALE DI GEOFISICA E VULCANOLOGIA

## Introduction

We apply two versions of the ETAS model and the Proximity to Past Earthquakes (PPE) model as the reference model to the Italian Seismic Instrumental and Parametric Database (ISIDE) of shallow seismicity collected by INGV for the 2009 L'Aquila seismic sequence that occurred in Abruzzi Region (Central Italy) (Figure 1) for the purpose of understanding the role of small events in forecasting large events. The data set spans from March 16, 2009 to June 30, 2009. We use the probability gain to evaluate their forecasting performance.

L'Aquila foreshock sequence, starting at the end of 2008 (with the largest event, Mw4.0, on March 30, 2009), was characterized by clustering around its mainshock (April 6, 2009, $M_w$6.3) nucleation area. Two other strong events with their own aftershocks occurred after the mainshock, on April 7, 2009 ($M_w$5.6) and April 9, 2009 ($M_w$5.4), respectively.

## Models for earthquake occurrences

### PPE (Proximity to Past Earthquakes) model

The PPE model is a Poisson model with a specific method of estimating the seismicity rate, i.e., it is a smoothed seismicity baseline model. It can play the role of a spatially varying reference model against which the performance of time-varying models can be compared. For this reason, it is adopted in this study as the reference model. It was proposed/formulated by Jackson and Kagan (1999) and named by Rhoades and Evison (2004).

$$\lambda(t,x,y,m) = \frac{s(m)}{t-t_0}\sum_{t_i<t}\left(\frac{a}{d^2+(x-x_i)^2+(y-y_i)^2}+\epsilon\right),\ m\geq m_c$$

$$s(m) = \beta e^{-\beta(m-m_c)},\ m\geq m_c$$

### Space-time ETAS models

Two versions of the ETAS model, named ETAS I and ETAS II, developed by different research groups, were used for evaluating the influence of small earthquakes on predictive performance. The difference between ETAS I and ETAS II is as follows.

ETAS I was developed by Ogata (1998) and Console et al. (2010a,b).

ETAS II was developed by Zhuang et al. (2005) and Ogata and Zhuang (2006), and is an improved version of the model in Ogata (1998).

Although these two versions belong to the same class of ETAS model, their details, such as how to determine background seismicity, how to deal with boundary conditions, and how to estimate parameters, are quite different.

Three versions of ETAS II are considered in order to understand the role of small events in forecasting large events, and to verify the statement made by Helmstetter (2003) and Helmstetter et al. (2005) that small events are important in triggering large earthquakes.

ETAS II-2.0+ (events of ≥M2.0)

ETAS II-1.6+ (events of ≥M1.6)

ETAS II-2.0m (events of M≥1.6 for calculating the expected number of events before t and auxiliary events with 1.6 ≤M≤2.0 for computing the likelihood).

We consider two forms for the spatial probability density function (p.d.f.):

ETAS I.
$$f(v,w;m) = \frac{q-1}{\pi D e^{\alpha(m-m_c)}}\left[1+\frac{v^2+w^2}{D e^{\alpha(m-m_c)}}\right]^{-q},$$

ETAS II.
$$f(v,w;m) = \frac{q-1}{\pi D e^{\gamma(m-m_c)}}\left[1+\frac{v^2+w^2}{D e^{\gamma(m-m_c)}}\right]^{-q}.$$

The parameters to be estimated in the learning phase by the maximum likelihood methods are: (A,α , c, p, D, q) for ETAS I and (A, α, c, p, D, q,γ) for ETAS II. In ETAS I, the scale factor for the aftershock productivity function is the same as the scaling factor for the spatial response function.

For ETAS I we assume α = 1.0·ln 10 for the physical meaning that the number of triggered events is proportional to the rupture area of the triggering earthquake (see Console et al., 2006; Hainzl et al., 2008).

A → Expected number of direct offspring produced by an event of the threshold magnitude

α → quantifies the difference in the productive efficiency from events of different magnitude

c and p → parameters in the Omori-Utsu formula for aftershock frequencies

D → characteristic triggering distance

q → spatial decay coefficient

γ → spatial scaling factor

## Data

The data used for this study are drawn from ISIDE. The periods April 16, 2005-March 15, 2009 and March 16, 2009-June 30, 2009 are used in the learning and test phases, respectively. The region to be tested with all the forecast models (i.e., 12.4°E–14.2°E ,41.5°N–43.1°N) is shown in Figure 1. The area of the learning is different for the ETAS models. For the ETAS I model is the same of the test, with 2,588 events (Mc ≥1.6, depth ≤ 30 km) in the learning period, while for ETAS II (7.9° E–18.7°E, 36.5°N–47.1°N). The data set for the test period contains 3,007 events (Mc ≥ 2.0, depth ≤ 30 km), occurred after the mainshock, on April 7, 2009 ($M_w$5.6) and April 9, 2009 ($M_w$5.4), respectively.

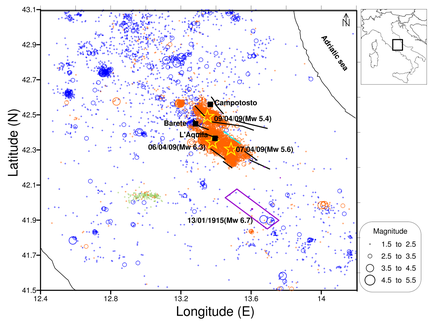


**Figure 1**

## Learning Phase

### PPE model

When fitting the PPE model to earthquake data, two cutoff magnitudes are used, 1.6 (2,588 events) and 2.0 (907 events), models PPE1.6+ and PPE2.0+, respectively, while the target events for both models are of magnitude 2.0 and higher.

| Model | $a$ | $d$ | $\epsilon$ | $\log L$ |
|---|---|---|---|---|
| | #(events) | $deg$ | #(events) | |
| PPE1.6+ | $9.542\times10^{-3}$ | $3.363\times10^{-3}$ | $6.469\times10^{-8}$ | -855.18 |
| PPE2.0+ | $1.497\times10^{-2}$ | $3.858\times10^{-3}$ | $3.360\times10^{-8}$ | -875.14 |

**Table 1.** Parameters of PPE models estimated by the maximum likelihood method (learning phase)

### ETAS I model

In the estimation of ETAS I, earthquake data (April 16, 2005-March 15, 2009, M≥1.6) from the L'Aquila area (12.4°E–14.2°E ,41.5°N–43.1°N) are used to obtain the seismicity rate.

### ETAS II model

In the estimation of ETAS II, earthquake data (April 16, 2005-March 15, 2009) from the region (7.9° E–18.7°E, 36.5°N–47.1°N) are used to obtain the seismicity rate. The events in this larger region with respect to the learning area of ETAS I are used as auxiliary events to incorporate the triggering effect from events outside into the contribution to the occurrence rate inside the L'Aquila area. That is, the events in this larger area are not considered in the likelihood computation. However, they are considered as events that could trigger other events inside the test area. This is a different point from ETAS I, arising from the independent development of these two models.

| Model | $A$ | $c$ | $\alpha$ | $p$ | $D$ | $q$ | $\gamma$ | $\beta$ |
|---|---|---|---|---|---|---|---|---|
| | #(events) | $day$ | | | $deg^2$ | | | |
| ETAS I | 0.2015 | 0.0202 | 2.30(fixed) | 1.10 | $2.13\times10^{-5}$ | 2.01 | n.a. | 2.58 |
| ETAS II-1.6+ | 0.642 | 0.00382 | 0.521 | 1.04 | $7.49\times10^{-5}$ | 1.73 | 0.910 | 2.60 |
| ETAS II-2.0+ | 0.453 | 0.00511 | 0.588 | 1.12 | $1.04\times10^{-4}$ | 1.73 | 0.755 | 2.60 |
| ETAS II-2.0m | 0.191 | 0.00396 | 1.140 | 1.09 | $7.93\times10^{-5}$ | 1.70 | 0.736 | 2.60 |

**Table 2.** Parameters of ETAS models estimated by the maximum likelihood method (learning phase)

## Daily Forecast

The area has been divided into cells of 1°x1°. As example we show a few daily forecasting maps by ETAS II-2.0m model given as the expected rate in each of cells for four time window (March 17, 2009, April 6, 2009, April 7, 2009, April 20, 2009). These forecasts consider the seismicity starting at 0:00 and ending at 24:00 (UTC) of each day (Figure2).

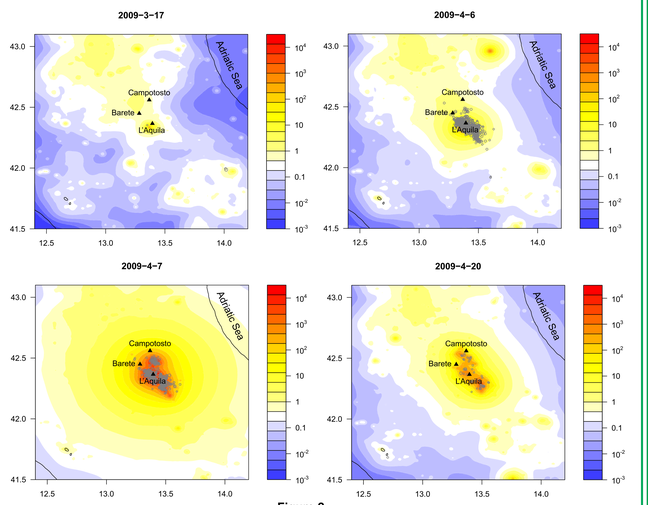


**Figure 2**

## Predictability of the mainshock

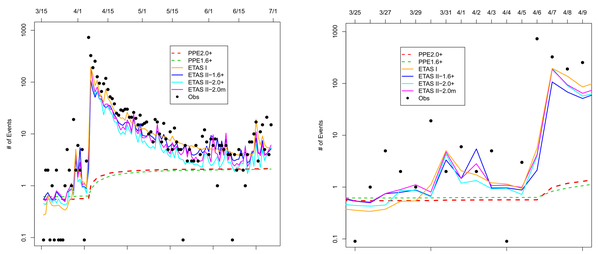


**Figure 3**

Figure 3 shows the occurrence rates forecast by all the models considered in this study, and the actual observations of daily number of earthquakes during the testing period starting on March 16, 2009. Among them, the PPE models start at a rate similar to that of the ETAS models, and with some increments in the forecast rates after the mainshock due to the dramatic increase of the number of events in the aftershock sequence. All the ETAS models catch the patterns of the temporal variation

of the aftershock rates with slight differences, except that the curve of earthquake numbers forecast by ETAS I is smoother than those produced by ETAS II

## Scoring procedures

Given forecasts from different models, it is important to know which model performs the best in forecasting. We only consider the information score, also called the entropy score to evaluate the performance of probability forecasts.

The whole space-time-magnitude window for a forecast is divided into cells of equal size. The forecast gives a probability pi that at least one event occurs in the ith space-time-magnitude cell; the reference model, is the Poisson model, which gives a probability of $\bar{p}_i$

The binomial information score is defined as the logarithm of the likelihood ratio of the forecasting and reference models:

$$B_i^{(b)} = Y_i \log(p_i/\bar{p}_i) + (1-Y_i)\log\frac{(1-p_i)}{(1-\bar{p}_i)},$$

The Poisson information score is defined by:

$$B_i^{(P)} = \sum_k I(n_i=k)\log(p_{i,k}/\bar{p}_{i,k}),$$

The information gain per unit space-time-magnitude volume is defined as:

$$G = \frac{\Delta}{V}\sum_{i=1}^{M} B_i,$$

V is the total volume of the space-time-magnitude range, $B_i$ takes on the value of $B_i^{(b)}$ or $B_i^{(p)}$, and $\Delta$ is the size of each cell. When $B_i$ takes on the value of $B_i^{(b)}$, G is called the binomial information gain. Similarly, G is the Poisson information gain when we use $B_i^{(p)}$.

| Model | $M2.0+$ | | | $M3.0+$ | | | $M4.0+$ | | |
|---|---|---|---|---|---|---|---|---|---|
| **Binomial information scores** | | | | | | | | | |
| | EC | NEC | Tot. | EC | NEC | Tot. | EC | NEC | Tot. |
| PPE1.6+ | 0.83 | 0.31 | 1.14 | 2.96 | -0.23 | 2.72 | 1.17 | -0.06 | 1.11 |
| ETAS I | 16.15 | -5.78 | 10.37 | 71.17 | -22.21 | 48.96 | 35.90 | -7.50 | **28.39** |
| ETAS II-1.6+ | 18.12 | -4.50 | 13.62 | 66.63 | -17.27 | 49.36 | 31.00 | -5.25 | 25.75 |
| ETAS II-2.0+ | 14.09 | -1.09 | 13.01 | 56.02 | -9.35 | 46.67 | 30.11 | -3.76 | 26.35 |
| ETAS II-2.0m | 17.87 | -3.43 | **14.44** | 64.81 | -14.71 | **50.10** | 32.13 | -5.08 | 27.05 |
| **Poisson information scores** | | | | | | | | | |
| | EC | NEC | Tot. | EC | NEC | Tot. | EC | NEC | Tot. |
| PPE1.6+ | 215.79 | 0.31 | 216.10 | 12.82 | -0.23 | 12.59 | 1.67 | -0.06 | 1.60 |
| ETAS I | 7992.22 | -5.78 | **7986.44** | 666.64 | -22.21 | **644.44** | 95.18 | -7.50 | **87.68** |
| ETAS II-1.6+ | 6860.19 | -4.50 | 6855.69 | 549.77 | -17.27 | 532.50 | 75.67 | -5.24 | 70.42 |
| ETAS II-2.0+ | 7322.93 | -1.08 | 7321.84 | 593.74 | -9.35 | 584.39 | 81.88 | -3.76 | 78.11 |
| ETAS II-2.0m | 7541.82 | -3.43 | 7541.82 | 617.48 | -14.71 | 602.77 | 85.19 | -5.08 | 80.11 |

**Table 3.** Information gain compared to Model PPE2.0+ for each model. The boldface fonts show the best models in the corresponding category. EC stands for "event cell" and NEC stands for "non-event cell"

## Discussion and Conclusions

· All the ETAS models used in this study underestimate the occurrence rate soon after the mainshock and during the aftershock sequence (Figure 3).

Two possible causes could be:

1) the ETAS models were fit to a learning data set of relatively moderate seismic activity, since there are no earthquakes of magnitude 5.0+ in the catalog before the test phase, March 15, 2009. In this case, our maximum likelihood (ML) parameters, applied to larger magnitude mainshocks, are in some sense the results of an extrapolation, which can easily cause large biases.

2) the ML parameters were not updated at the end of each day, just before the computation of a new forecast for the following day. This would improve the performance of an ETAS model, especially in the case of a long aftershock sequence.

· Comparing the two types of ETAS models: 1) ETAS I (with the same fixed exponent coefficient α = 2.3 for both the productivity function and the scaling factor in the spatial response function) performs better in forecasting the active aftershock sequence than the ETAS II-type models, when the Poisson score is adopted; 2) Before the mainshock all ETAS II models performed better than ETAS I.

· The occurrence of foreshock activity some days before the mainshock raised the probability gain up to an order of 20, using the ETAS I model. This does not appear to be a great achievement towards the potential use of this information for civil protection purposes.

· We do not consider the performance of these models in forecasting spatial locations, since the area is quite small, 1.1° by 1.5°, while the location error is several kilometers. Moreover, all the models use the G-R magnitude-frequency relation for the magnitude distribution, independent of the time and location components. Thus, there are no differences between these Etas models in forecasting the magnitude distribution of future events.

In summary, to achieve better forecasts, as well-known from the existing literature on the ETAS model, the training catalog should contain some typical examples of magnitudes similar to that of the mainshock. If not, it would be better to use a typical set of parameters from a nearby region or from a region of similar tectonic structure or equivalent seismicity levels. Other lessons from this study are as follows. (1) Making use of the earthquakes of lower magnitude works better than using only events larger than the target magnitude threshold. (2) Parameters should be updated during the forecast process, if possible. (3) Forecasts should be updated just after the occurrence of potential foreshock activity, whenever significant moderate earthquakes are observed.

### References

Console, R., Murru, M., and Catalli, F. (2006). Physical and stochastic models of earthquake clustering. Tectonophysics, 417:141–153.
Console, R., Murru, M., and Falcone, G. (2010a). Probability gains of an epidemic-type aftershock sequence model in retrospective forecasting of m > 5 earthquake in Italy. Journal of Seismology, 14(1):9–26.
Console, R., Murru, M., and Falcone, G. (2010b). Retrospective forecasting of m > 4.0 earthquakes in New Zealand. Pure and Applied Geophysics, 167:693–707. 10.1007/s00024-010-0068-2.
Hainzl, S., Christophersen, A., and Enescu, B. (2008). Impact of earthquake rupture extensions on parameter estimations of point-process models. Bull. Seismol. Soc. Am., 98(4):2066–2072.
Helmstetter, A. (2003). Is earthquake triggering driven by small earthquakes? Phys. Rev. Lett., 91(5):058501.
Helmstetter, A., Kagan, Y. Y., and Jackson, D. D. (2005). Importance of small earthquakes for stress transfers and earthquake triggering. Journal of Geophysical Research, 110.
Jackson, D. D. and Kagan, Y. Y. (1999). Testable earthquake forecasts for 1999. Seismological Research Letters, 70:393–403.
Ogata, Y. (1998). Space-time point-process models for earthquake occurrences. Annals of the Institute of Statistical Mathematics, 50:379–402.
Ogata, Y. and Zhuang, J. (2006). Space-time ETAS models and an improved extension. Tectonophysics, 413(1-2):13–23.
Rhoades, D. A. and Evison, F. F. (2004). Long-range earthquake forecasting with every earthquake a precursor according to scale. Pure and Applied Geophysics, 161:47–72.
Zhuang, J., Chang, C.-P., Ogata, Y., and Chen, Y.-I. (2005). A study on the background and clustering seismicity in the Taiwan region by using a point process model. Journal of Geophysical Research, 110:B05S13.